

GSA DATA REPOSITORY 2014372

From continent to intra-oceanic arc: zircon xenocrysts record the crustal evolution of the Solomon Island Arc

Simon Tapster¹, N.M.W Roberts, M.G Petterson, A.D Saunders, J Naden

¹Corresponding author email: Simont@bgs.ac.uk

CONTENTS:

Methods and analytical techniques

- Mineral separation
- Zircon Imaging
- U-Pb Geochronology
- Critically appraising the risk of contamination
- Methods bias in the age frequency distribution
- Reproducibility of results

Figure DR1

- Cathodoluminescence (CL) images, spot locations and ages of representative zircons from age populations.

Figure DR2

- Extended figure 2, caption and references

Figure DR3

- **A:** Tera-Wasserburg diagram for sample X002 titanite U-Pb data.
- **B:** Tera-Wasserburg diagram for sample UM13B rutile U-Pb data.
- **C:** U-Pb zircon age distributions for magmatic emplacement populations.
- **D:** U-Pb zircon age distributions for ca 95 Ma populations.
- **E:** Individual sample zircon age frequency histograms

Table DR1. Hand Sample locations and descriptions

Table DR2. Zircon, titanite and rutile LA-ICPMS U-Pb data

METHODS AND ANALYTICAL TECHNIQUES

Mineral separation

Mineral separation was carried out at the NERC Isotope Geosciences Laboratory (NIGL). The general stages after sample washing were jaw crushing, disc milling and sieving (<355 µm). Heavy minerals were concentrated using a Rodgers Table, Frantz electromagnetic separator and MI heavy liquids (diiodomethane). Extensive efforts to ensure cleanliness were maintained throughout. Heavy minerals were then handpicked in alcohol under a binocular microscope with attempts to retrieve the full zircon fraction. Zircons, rutile and titanite were mounted in epoxy and polished with ¼ µm diamond paste to near-equatorial sections.

The total mass of each sample used within the extractions was variable, and ranged from ~1 kg for X008, ~4 kg for UM14B and UM13B, and ~6 kg for X002.

See *Reproducibility of results* section for further details on mineral separations

Zircon Imaging

Cathodoluminescence imaging of zircon internal structures in polished epoxy mounts was carried out at the University of Leicester using a Hitachi S-3600N scanning electron microscope with a GATAN PanaCL ellipsoidal mirror plate inserted. Operating conditions for the SEM were 15 kV, 50 µA and an 11-13 mm working distance.

U-Pb Geochronology

Zircons were analysed for U-Pb geochronology using a Nu Instruments Attom HR single-collector inductively coupled plasma mass spectrometer (HR-ICP-MS). Laser ablation was performed with a New Wave Research UP193ss laser ablation system, using a ‘large-format’ New Wave Research cell; this features a moveable cup with an ablation volume of ca. 3-4 cm³, which combined with <1m tubing to the plasma torch leads to a washout time of < 1 second. The ablation parameters were a 25µm static spot, a repetition rate of 5Hz, a fluence of 1.5 to 2.5 j/cm², a 15 second washout period between analyses, and a 30 second ablation time. Tuning was adopted that gave a ThO of <0.4%, and UO of <0.1%. Data processing used the time-resolved function on the Nu Instruments’ software, an in-house Excel spreadsheet for data reduction and error propagation, and Isoplot for data presentation (Ludwig, 2003). All data are plotted at the 2σ confidence interval.

The Nu Attom HR-ICP-MS is used in peak-jumping mode with measurement on a MassCom secondary electron multiplier. The following masses are measured in each sweep: ²⁰²Hg, ²⁰⁴Pb+Hg, ²⁰⁶Pb, ²⁰⁷Pb, ²⁰⁸Pb, ²³²Th, and ²³⁵U. Each data integration records 100 sweeps of the measured masses, which roughly equates to 0.22 seconds. Dwell times on each mass are 500µs on ²⁰⁷Pb and ²³⁵U, and 200µs on all other masses; the switching between masses takes 40µs. Since ²³⁵U is measured, ²³⁸U is calculated from ²³⁵U *137.818.

A standard-sample-bracketing technique was used to correct the data, which involved calculation of normalization factors based on the measured/accepted value for the $^{207}\text{Pb}/^{206}\text{Pb}$ and $^{206}\text{Pb}/^{238}\text{U}$ ratios of a zircon reference material, analysed at regular intervals during each session; two other zircon reference materials were analysed during each session to check for accuracy and precision of the method. Since many of the zircons contained a small component of common lead, a correction was made so that accurate $^{206}\text{Pb}/^{238}\text{U}$ ages could be given for the young (<600 Ma) zircons. A ^{207}Pb based correction was used, that utilizes the measured $^{207}\text{Pb}/^{206}\text{Pb}$ ratios, and an assumed $^{207}\text{Pb}/^{206}\text{Pb}$ ratio of common lead to calculate the proportion of common ^{206}Pb ; this correction assumes that the U-Pb data are concordant, but is useful in young grains where accurate knowledge of the $^{206}\text{Pb}/^{238}\text{U}$ is required. For common lead, the Stacey & Kramers (1975) model composition is used, and an initial age estimate is based on regression in a Tera-Wasserburg diagram. A correction is also made to the common-lead corrected ages to account for any deficit in ^{206}Pb that is derived from the initial exclusion of ^{230}Th , an intermediate daughter nuclide of the ^{238}U decay series, during zircon crystallisation. This correction is relatively minor in zircon, titanite and rutile, because Th/U ratios are low; above ages of 10 Ma the correction is <1%, and above 100 Ma is < 0.02%. An estimated value of 3 was used for the melt Th/U ratio in this case.

Propagated uncertainties include the internal uncertainty, i.e. the reproducibility of the measured ratios during an ablation, and an external uncertainty, i.e. the reproducibility of the bracketing reference material during a session; these were added in quadrature.

Titanite and rutile were measured using the same protocol as for zircon; normalisation involved standard bracketing with matrix-matched reference materials.

Standards									
Date	Material	1° standard	Pb/U 2sd%	2° standard	Pb/U age	Pb/U 2sd%	3° standard	Pb/U age	Pb/U 2sd%
25/06/2012	Zircon	91500	3.0	GJ-1	602 ± 14	2.3	Mud Tank	736 ± 25	3.4
26/06/2012	Zircon	91500	2.9	GJ-2	602 ± 16	2.6	Mud Tank	736 ± 22	3.0
27/06/2012	Zircon	91500	2.7	GJ-3	604 ± 26	4.3	Mud Tank	745 ± 21	2.8
06/08/2012	Zircon	91500	2.4	GJ-4	604 ± 10	1.6	Mud Tank	733 ± 15	2.0
07/08/2012	Zircon	91500	2.9	GJ-5	604 ± 12	2.1	Mud Tank	730 ± 19	2.6
08/08/2012	Zircon	91500	2.5	GJ-6	603 ± 14	2.2	Mud Tank	731 ± 20	2.7
08/08/2012	Rutile	R10	3.4	R19	488 ± 24	4.9			
08/08/2012	Titanite	Ont2	2.0	Khan	525 ± 15	2.9			

Laboratory & Sample Preparation	
Laboratory name	NERC Isotope Geosciences Laboratory
Sample type/mineral	Zircon, titanite, rutile
Sample preparation	Conventional mineral separation, 1 inch resin mount, 1/4µm polish to finish
Imaging	Cathodoluminescence
Laser ablation system	
Make, Model & type	ESI/New Wave Research, UP193SS
Ablation cell & volume	NWR two-volume 'large format cell' with low effective volume (ca. 3-4cm ³), washout time ca.1sec
Laser wavelength (nm)	193nm
Pulse width (ns)	3-4ns
Fluence (J.cm ⁻²)	1.5-2.5 J.cm ⁻²
Repetition rate (Hz)	5Hz
Ablation duration (secs)	30secs
Ablation pit depth / ablation rate	~15µm pit depth, measured using an optical microscope
Spot size (µm)	25µm
Sampling mode / pattern	Static spot ablation
Carrier gas	100% He, Ar make-up gas combined ca.50% along sample line.
Cell carrier gas flow (l/min)	0.7l/min
ICP-MS Instrument	
Make, Model & type	Nu Instruments Attom SC-SF-ICP-MS
Sample introduction	Free air aspiration of desolvator
RF power (W)	1300W
Make-up gas flow (l/min)	0.8l/min Ar
Detection system	Discrete dynode MassCom ion counter
Masses measured	202, 204, 206, 207, 208, 232, 235
Integration time per peak (ms)	Ca.200ms
Total integration time per reading (secs)	Ca.1 sec
Sensitivity / Efficiency (%, element)	Not measured
IC Dead time (ns)	15ns
Data Processing	
Gas blank	60 second on-peak zero subtracted
Calibration strategy	91500, GJ1 & Mud Tank (zircon); Ontario-2 & Khan (titanite); R10 & R19 (rutile). One used as primary reference material for normalization, and others used as check on accuracy.
Reference Material info	91500 (1065 Ma; Wiedenbeck et al. 1995) Mud Tank (732 ± 1 Ma; in-house TIMS) GJ1 ($^{206}\text{Pb}/^{238}\text{U}$ 602.3 ± 1 Ma, $^{207}\text{Pb}/^{206}\text{Pb}$ 609.2 ± 0.7 Ma; in-house TIMS, – see also Jackson et al. 2004) Ontario-2 (1054 ± 2 Ma; in-house TIMS) Khan (522 Ma; in-house TIMS) R10 (1089 ± 2 Ma; in-house TIMS, – see also Luvizotto et al. 2011) R19 (489 ± 0.9 Ma; Zack et al. 2011)
Data processing package used / Correction for LIEF	Nu Instruments TRA acquisition software, in-house spreadsheet data processing
Mass discrimination	$^{207}\text{Pb}/^{206}\text{Pb}$ and $^{206}\text{Pb}/^{238}\text{U}$ normalised to reference material
Common-Pb correction, composition and uncertainty	Stacey & Kramers (1975) model composition, based on f206c, using estimated age derived from $^{206}\text{Pb}/^{238}\text{U}$.
Uncertainty level & propagation	Ages in the data table are quoted at 2sigma absolute, propagation is by quadratic addition. Reproducibility of reference material is propagated.
Quality control / Validation	See data table for validation results

Critically appraising the risk of contamination

Given the nature of the findings, the risk of laboratory contamination (addition of external zircon crystals unrelated to the samples before U-Pb analysis) is a concern and requires critical appraisal.

Immediately upon the disaggregation of a whole rock sample through geological or anthropogenic means, the risk of contamination is introduced and can never be eliminated no matter what precautions are taken. This risk concerns all crystals regardless of their age, although a greater weighting of confidence may be placed in dates that are in agreement with the expected age of a sample, e.g. a magmatic emplacement age. Unlike the zircons of our study, xenocrysts are commonly identified as older cores with younger rims that correspond in age to their associated intrusion, giving confidence to a relationship between the magmatic system and the source of older zircons. However, the absence of rims alone does not signify contamination. Natural samples within magmatic systems which display both populations of young grains and xenocystic zircons without young rims have been previously observed in an island arc setting (Reddy et al., 2009). Enclaving of zircons in xenoliths, refractory xenocrysts and minerals that crystallising from magma prior to zircon saturation may all prohibit the growth of young zircon rims growing around old cores or their complete dissolution into the melt.

The small, heavily vegetated, tropically weathered and hydrothermally altered exposures in the Umasani area placed severe constraints on the identification of features that appear foreign in hand sample or thin section. Basaltic xenoliths were observed at the sample location of X002 and have been previously been described within early intrusive phases of the Umasani and Poha plutonic complexes (Hackman, 1979). However, further detailed investigations are needed to ascertain xenolith affinity and if they bear xenocrysts.

Only by identifying the full range in zircon age populations truly in-situ (i.e. prior to disaggregation), can the risk of contamination be entirely negated. However, in many instances a grain by grain, in-situ analysis of thin section zircons is unfeasible owing to the relatively sparse nature of accessory zircon in natural samples (in particular xenocystic zircon in this instance) and the low volume of rock that can be intensively examined. From the ~15 kg of bulk rock that was processed within this study, only ~100 xenocrysts were identified. The number of initial xenocrysts may well exceed this; yet the low zircon yield is a reflection upon the low density within the initial sample. Heterogeneity in the physical distribution of zircons and their ages may also occur within the bulk rock on a scale not resolvable within thin section. The poor representation of zircons in a thin section may therefore lead to a deficit of geological complexity from the resulting geochronology of a sample. In part, this is why processing high volume samples through heavy mineral separations is commonly more favourable for producing representative U-Pb ages for a rock.

Methods bias in the age frequency distribution

Even within high volume samples, initial bias of zircon analysed U-Pb dates may be introduced by natural heterogeneities within a sample selected for mineral separation. These include the variation in concentration and distributions of zircon age populations and the volume of whole rock used.

Traditional heavy mineral separation methods are not closed systems. Rather, they concentrate heavy minerals, thus different size and morphological fractions may be preferentially lost during their processing (c.f. Sláma and Košler, 2012). The liberation of zircon grains from bulk rock using crushing techniques adds an additional factor of bias in comparison to detrital zircon mineral extractions from unconsolidated sediment samples.

Human selection bias during hand picking under a binocular microscope may also have considerable impact on the ages of the final zircons analysed in preference of those with larger grain sizes (e.g. Sláma and Košler, 2012). While we made every attempt to retrieve the full zircon fraction no guarantee can be made to the extent of missed grains or those lost during transfer and mounting.

It is in our opinion that the frequency distribution of age data for a given sample is not necessarily representative of the age frequency distributions of the initial zircon population. The age distribution is perhaps more reliable, although the absence of zircon dates does not necessarily indicate the absence of that age of zircons from the samples or the crust of Guadalcanal.

Reproducibility of results

As the possibility of sample contamination can never be entirely ruled out from a heavy mineral separate, an important test is the ability to independently reproduce age results. In discussing the origins of zircon xenocrysts within the Arabian-Nubian Shield, Stern et al. (2010) present the reproducibility of xenocryst grain ages from heavy mineral separations in three different laboratories as the core argument against a laboratory contamination source. We have ensured reproducibility within our results across several relevant points, which we describe below with further details of mineral separation methodology.

Heavy minerals were first extracted from sample X002. The initial separation yielded only several zircons visible under a binocular microscope and warranted re-sampling from the field. Zircons were extracted from a second, larger hand sample of X002 during the same run of samples as an aliquot of UM13B (UM13B-1). On both occasions samples were passed twice across a Rodgers Table before Frantz and heavy liquid separation. The zircons yielded by the two extractions of X002 were mixed before mounting in epoxy.

Nine months after extractions of X002 and UM13B-1, we processed samples UM14B, X008 and a second aliquot of UM13B (UM13B-2). Aliquots of UM13B remained isolated from each other throughout all stages.

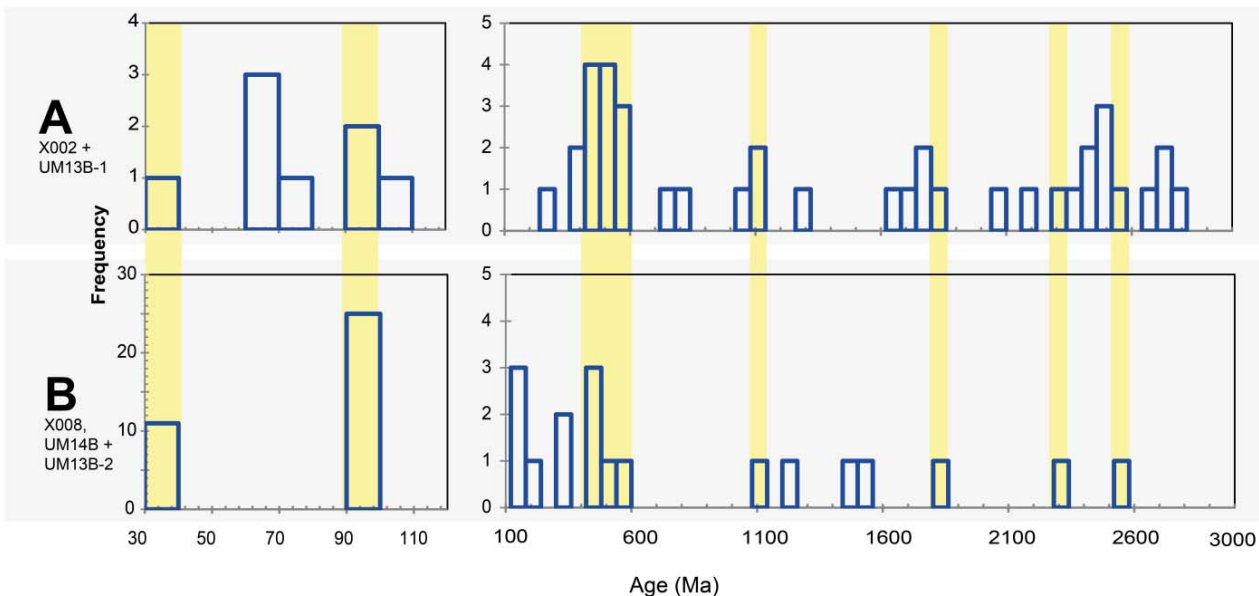
In order to avoid the possibility of zircon adhered to the external surfaces, samples of X008, UM14B and UM13B-2 were thoroughly washed and sealed until crushing. Crushing apparatus was cleaned to the high standards maintained throughout procedures, and a portion of UM14B was used to self-contaminate all crushing and sieving equipment before being discarded. The sample of UM14B from which we analysed zircons from, was then processed and apparatus was again cleaned between each of the following sample runs of X008 and UM13B-2. To maximise the zircon yield, samples were passed only once over the Rodger's Table before concentration using a Frantz electromagnetic separator and heavy liquids.

During the two sessions of mineral separation in November 2011 and July 2012 an additional 23 samples from Miocene or younger igneous units of the Solomon Islands were also processed using the same methods and apparatus. These samples either bracketed or occurred as intervals between runs of the Umasani samples of this study, and therefore act as controls within our experiments.

The temporal gap between sessions of heavy mineral separation creates some independence between experiments. Figure 1 shows ages across the spectra were reproduced by the mineral extractions after a 9 month period. Zircon dates older than Oligocene, occurred in both aliquots of UM13B that were independently separated.

The large range in ages that were reproduced during both separations also indicates that if zircons were an artefact of contamination it would be unlikely to be derived from a single contaminant source; therefore persistent laboratory contamination from a similar mixture of samples would need to be present over this 9 month time period.

If persistent contamination occurred over a prolonged period we may expect similar ages of zircons to be present throughout the additional 23 samples that bracketed xenocryst bearing samples in the run of separations, they are not. Of 16 other bulk samples prepared and analysed during the same November 2011 and July 2012 sessions as xenocryst bearing samples (>600 zircon CL images and >300 individual LA-ICP-MS U-Pb analyses) no similar internal textures were identified and all returned ages younger than the zircons discussed within this study. It is noteworthy, given a possible bias during hand picking, that these analyses include grains of a similar size fraction to xenocrysts zircons. In a further 7 samples, zircon was either completely absent (blanks) or gave low zircon yields (<20 grains) which are optically different from the xenocrystic grains under a binocular microscope. Zircon grains older than the Oligocene were only identified in the heavy mineral separates of the same litho-chemical intrusive unit from the Umasani area.



Age frequency distributions of xenocrysts identified in mineral separations conducted in (A) August and November 2011 and (B) July 2012. Reoccurring zircon dates are highlighted in yellow. Reproducibility of zircon dates occurs throughout the age spectrum.

Additionally, Umasani samples processed within in the same session of extraction did not yield the same age distribution. The clearest example is of the July 2012 extraction from which X008 only yielded one Eocene aged grain, whereas UM14B and UM13B-2 which bracketed X008 yielded much older grains (Fig. DR3, Table DR2). It is difficult to reconcile persistent laboratory contamination over 9 months with the intermittent occurrence of older zircons from one sample to the next, and the selective contamination of samples from the same intrusive complex only.

As a further test, the remaining hand sample material of X002 was processed in April 2013. To decrease the risk of contamination from crushing equipment, a ~5 cm diameter tightly fitting tungsten carbide piston and hammer was used to crush the sample from hand sample to powder. Before contact with the sample, the piston was thoroughly cleaned and its inner surfaces were examined under a binocular microscope to ensure it was free from residual material. The sample was sieved to <355 µm. Fines were removed by washing the sample in a 5L glass beaker rather than Rodger's table, before electromagnetic and heavy liquid separation. Importantly, a Pliocene gabbro control sample containing Zr 8 ppm (XRF analysis, unpublished data) was processed through each stage of the separation immediately before X002 (apparatus was thoroughly cleaned in between samples).

Unmounted zircon from the April 2013 extraction of X002 again yielded 3 zircons with Archean, Proterozoic and Late Cretaceous dates (data are not included within the presented data set and are available upon request from the corresponding author). The heavy mineral separate of the Pliocene gabbro control (processed through the apparatus first) showed no evidence of zircon under the same optical microscope conditions as X002. We deem this as further evidence that the older zircons are xenocrysts contained within the Umasani samples.

While the possibility of contamination cannot be refuted, the procedures and reproducibility ensure a high level of confidence in the results not being an artefact of laboratory contamination.

REFERENCES CITED

- Hackman, B., 1979, Geology of the Honiara area, Solomon Islands Geological Survey Division. Bulletin no.3, p. 1–46.
- Jackson, S.E., Pearson, N.J., Griffin, W.L., Belousova, E.A. 2004. The application of laser ablation-inductively coupled plasma-mass spectrometry to in situ U-Pb zircon geochronology. *Chemical Geology* 211, 47-69.
- Ludwig, K.R., 2003. User's Manual for Isoplot 3.00: A Geochronological Toolkit for Microsoft Excel; Berkeley Geochronology Center Special Publication; no. 4, Berkeley, California.
- Luvizotto, G.L., Zack, T., Meyer, H.P., Ludwig, T., Triebold, S., Kronz, A., Münker, C., Stockli, D.F., Prowatke, S., Klemme, S., Jacob, D.E., von Eynatten, H. 2009. Rutile crystals as potential trace element and isotope mineral standards for microanalysis. *Chemical Geology* 261, 346-369.
- Reddy, S. M., Timms, N. E., Hamilton, P. J., & Smyth, H. R. (2009). Deformation-related microstructures in magmatic zircon and implications for diffusion. *Contributions to Mineralogy and Petrology*, 157(2), 231-244.
- Schmitz, M., Bowring, S.A. 2001. U-Pb zircon and titanite systematics of the Fish Canyon Tuff: an assessment of high-precision U-Pb geochronology and its application to young volcanic rocks. *Geochimica et Cosmochimica Acta* 65, 2571-2587.
- Sláma, J., & Košler, J. 2012. Effects of sampling and mineral separation on accuracy of detrital zircon studies. *Geochemistry Geophysics Geosystems*, 13(null), Q05007.
- Smyth, H. R., Hamilton, P. J., Hall, R., & Kinny, P. D. (2007). The deep crust beneath island arcs: Inherited zircons reveal a Gondwana continental fragment beneath East Java, Indonesia. *Earth and Planetary Science Letters*, 258(1), 269-282.
- Stacey, J.S., Kramers, J.D. 1975. Approximation of terrestrial lead isotope evolution by a two-stage model. *Earth and Planetary Science Letters* 26, 207–221.
- Stern, R. J., Ali, K. A., Liégeois, J. P., Johnson, P. R., Kozdroj, W., & Kattan, F. H. (2010). Distribution and significance of pre-Neoproterozoic zircons in juvenile Neoproterozoic igneous rocks of the Arabian-Nubian Shield. *American Journal of Science*, 310(9), 791-811.
- Wiedenbeck, M., Allé, P., Corfu, F., Griffin, W.L., Meier, M., Oberli, F., von Quadt, A., Roddick, J.C., Spiegel, W. 1995. Three natural zircon standards for U-Th-Pb, Lu-Hf, trace element and REE analyses. *Geostandards Newsletter* 19, 1-23.
- Zack, T., Stockli, D.F., Luvizotto, G.L., Barth, M.G., Belousova, E., Wolfe, M.R., Hinton, R.W. 2011. In situ U-Pb rutile dating by LA-ICP-MS: ^{208}Pb correction and prospects for geological applications. *Contributions to Mineralogy and Petrology* 162, 515-530.

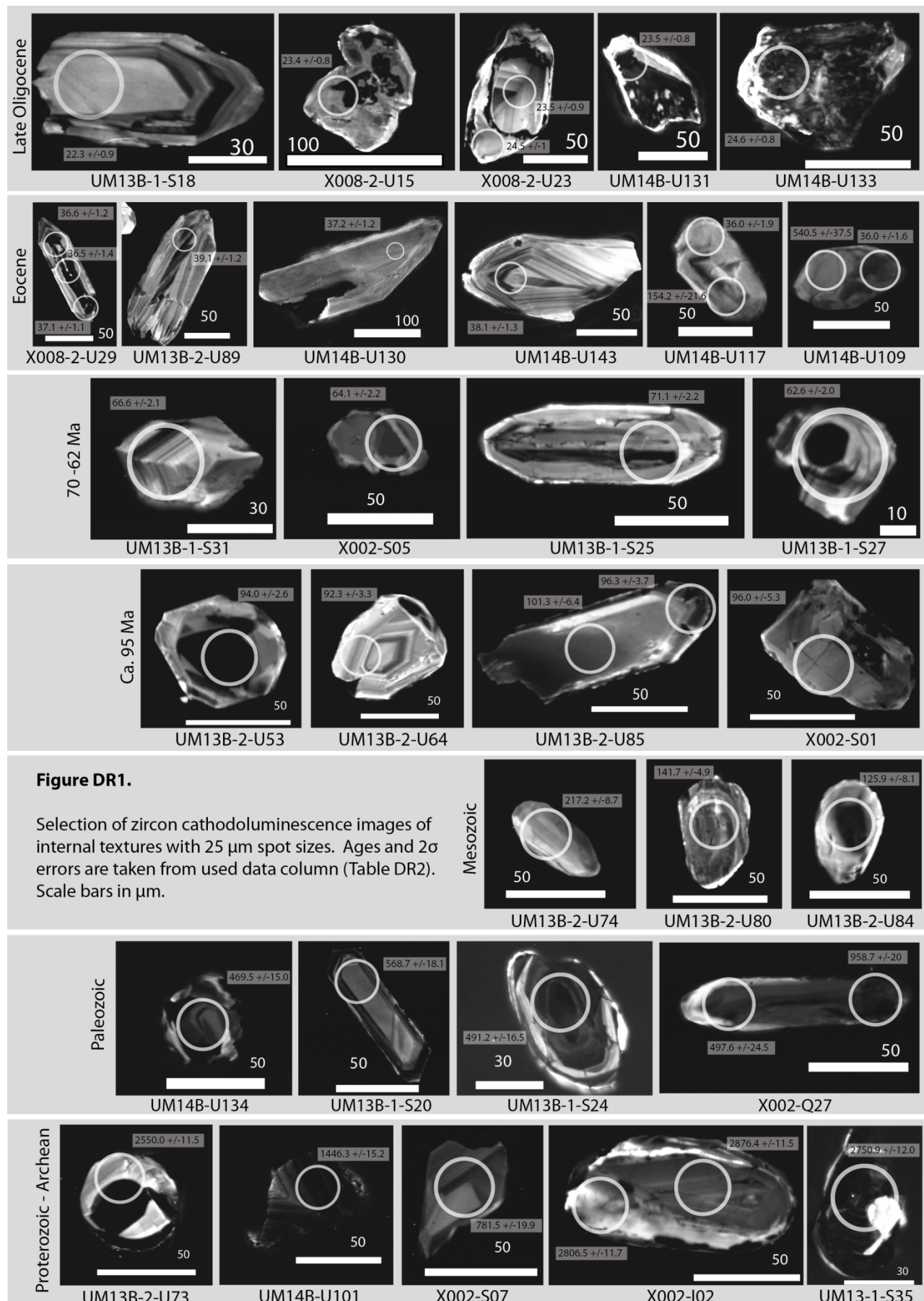


Figure DR1.

Selection of zircon cathodoluminescence images of internal textures with 25 μm spot sizes. Ages and 2σ errors are taken from used data column (Table DR2). Scale bars in μm .

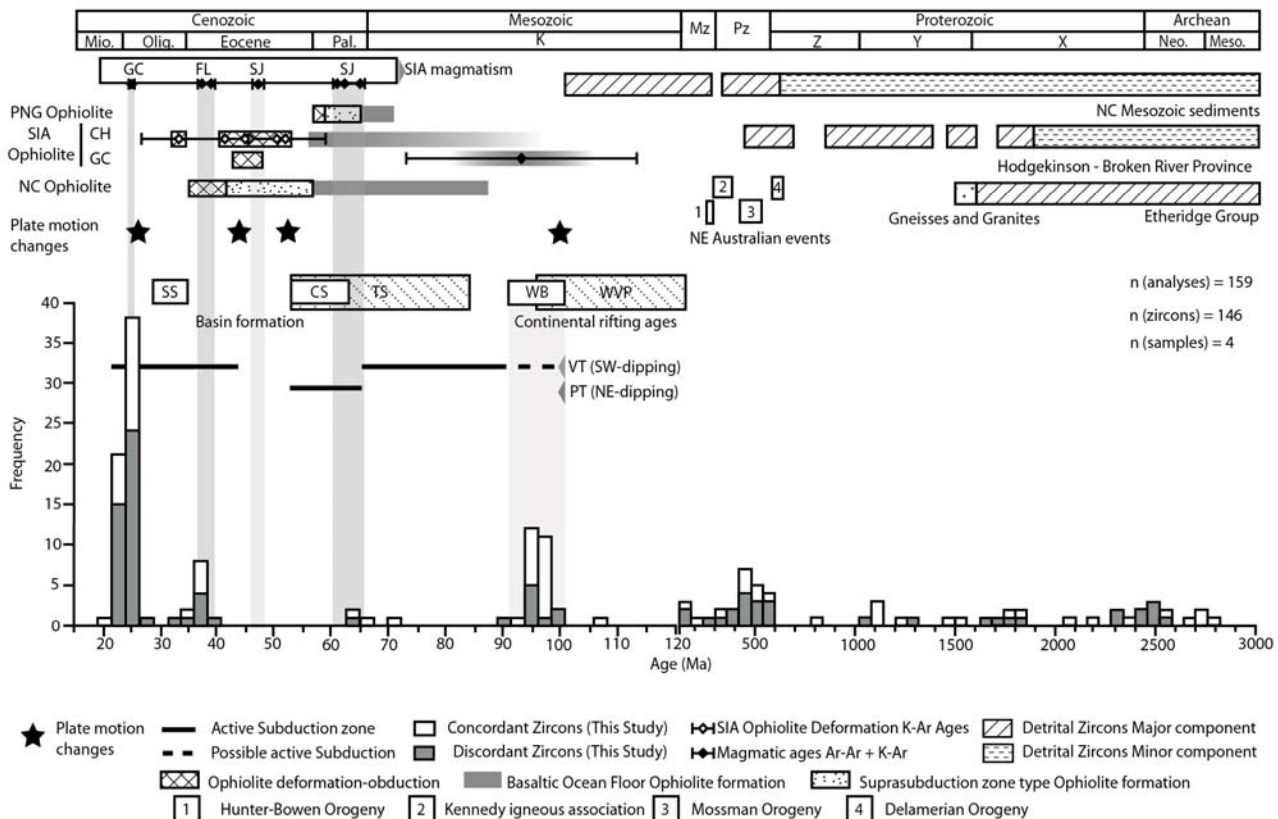


Figure DR2. Frequency histogram of zircon ages from the Umasani Pluton and extended summary of corresponding regional tectonic events and zircon ages. Inherited ages in the arc are similar to NE Australian and New Caledonian detrital zircons >120 Ma and the ages for magmatic arc units that alternate with basin formation since the Late Cretaceous continental rifting events. Concordant ages (>90% concordance), discordant ages (<90% concordance). Histogram bins <120 Ma represent 2 Ma, >120 Ma bins represent 60 Ma. $^{206}\text{Pb}/^{238}\text{U}$ Ages are used for <600 Ma, $^{207}\text{Pb}/^{206}\text{Pb}$ ages are used for older zircons.

Abbreviations: CH - Choiseul Island; CS - Coral Sea; FL - Florida Islands; GC - Guadalcanal; LHR - Lord Howe Rise; LP - Louisiade Plateau; NC - New Caledonia; OJP - Ontong Java Plateau; PNG – Papua New Guinea; PT - Pocklington Trough relict subduction zone; SIA - Solomon Island Arc; SJ - San Jorge Volcanics (contained within the Jajao igneous complex - JJ); SS - Solomon Sea; TS - Tasman Sea; VT - Vitiaz Trench; WB - Woodlark Basin. WVP - Whitsunday Volcanic Province.

Presented ages of events in overlay are as follows:

Guadalcanal ophiolite formation 92 ± 20 Ma (K-Ar; Snelling et al., 1970) and stratigraphic mid-Eocene deformation ages (Hackman 1980). Choiseul Island ophiolite formation stratigraphic age (Ridgway et al., 1987) and range of deformation K-Ar ages (Richards and Cooper, 1966).

Timings for the formation and emplacement of the Papua New Guinea and New Caledonian ophiolite (Whattam et al., 2008 and references therein; Whattam, 2009 and references therein). Note that the deformation ages for the Solomon Island Arc ophiolite deformation lies in between

that of PNG and New Caledonia, in keeping with the southwards younging disrupted ophiolite belt of Parrot and Dugas (1980) and Whattam (2009). Within the other cases of ophiolite formation along the SW Pacific margin, Whattam (2009) identifies that the genesis of ophiolite crust occurs in a supra-subduction zone environment, following formation in a back-arc basin environment represented by the basaltic ocean floor symbol. Emplacement of both types of basaltic crust as ophiolite occurs due to the partial subduction and rebound of micro-continental ribbons at short lived N to E dipping subduction zones.

Spreading ages of the Solomon Sea (magnetic anomalies; Joshima et al., 1986) and Coral Sea (magnetic anomalies; Weissel and Watts, 1979; Gaina et al., 1999). Ages for continental rift related magmatism associated with the break-up of Eastern Gondwana are for the Whitsunday Volcanic Province, 132–95 Ma (Rb-Sr and K-Ar; Bryan et al., 1997 and references therein.) and 100–90 Ma zircons from the Woodlark Basin rift (U-Pb; Zirakparvar et al., 2013). Tasman Sea spreading (Schellart et al., 2006 and references therein.).

Ages of Solomon Island Arc magmatism are for arc-BAB San Jorge Volcanics of the Jajao Igneous complex 61–64 Ma and 46 Ma (Ar-Ar; Tejada et al., 1996), Florida Island volcanic basement sequence including gabbros and tonalites at 45–37 Ma (K-Ar; Neef and McDougall, 1976) and the Poha tonalite 24.4 ± 0.4 Ma (K-Ar; Chivas and McDougall, 1978).

Subduction zone activity for the Vitiaz trench and Pocklington Trough (Schellart et al., 2006; Whattam et al., 2008; Whattam, 2009 and references therein.).

Plate motion changes are at 26–23 Ma (Knesel et al., 2008), 43 Ma and 99 Ma (Vevers, 2000), and 53–50 Ma (Whittaker et al., 2007). Note that continental rifting and the onset of extensional ophiolite crust formation is preceded by major tectonic change, just as the ophiolite deformation in the SIA is bracketed by two major tectonic reorganisation events.

Ages for zircon forming North-Eastern Australian orogenies and events (Withnall and Henderson, 2012). Detrital zircon age ranges from Teremba, Boghen and Central Mesozoic terrane sediments of New Caledonia (Adams et al., 2009); Hodgkinson-Broken River Provinces (Fergusson et al., 2007); Etheridge Group Metasediments and granites and gneiss ages within the area (Neumann and Kositcin, 2011). Major detrital component refers to dominant peaks in probability density functions where as minor component indicates dates or uncertainties present across the age range.

REFERENCES CITED

- Adams, C., Cluzel, D., and Griffin, W., 2009, Detrital-zircon ages and geochemistry of sedimentary rocks in basement Mesozoic terranes and their cover rocks in New Caledonia, and provenances at the Eastern Gondwanaland margin*: Australian Journal of Earth Sciences, v. 56, no. 8, p. 1023-1047.
- Bryan, S., Constantine, A., Stephens, C., Ewart, A., Schön, R., and Parianos, J., 1997, Early Cretaceous volcano-sedimentary successions along the eastern Australian continental margin: Implications for the break-up of eastern Gondwana: Earth and Planetary Science Letters, v. 153, no. 1, p. 85-102.

- Chivas, A.R., and McDougall, I., 1978, Geochronology of Koloula-Porphyry-Copper-Prospect, Guadalcanal, Solomon-Islands: *Economic Geology*, v. 73, no. 5, p. 678-689.
- Fergusson, C.L., Henderson, R.A., Fanning, C.M., and Withnall, I.W., 2007, Detrital zircon ages in Neoproterozoic to Ordovician siliciclastic rocks, northeastern Australia: implications for the tectonic history of the East Gondwana continental margin: *Journal of the Geological Society*, v. 164, no. 1, p. 215-225.
- Gaina, C., Muller, R., Royer, J., and Symonds, P., 1999, Evolution of the Louisiade triple junction: *Journal of Geophysical Research-Solid Earth*, v. 104, no. B6, p. 12927-12939.
- Joshima, M., Okuda, Y., Murakami, F., Kishimoto, K., and Honza, E., 1986, Age of the Solomon Sea Basin from magnetic lineations: *Geo-Marine Letters*, v. 6, no. 4, p. 229-234.
- Knesel, K.M., Cohen, B.E., Vasconcelos, P.M., and Thiede, D.S., 2008, Rapid change in drift of the Australian plate records collision with Ontong Java plateau: *Nature*, v. 454, no. 7205, p. 754-757.
- Neumann, N.L., and Kositcin, N., 2011, New SHRIMP U-Pb zircon ages from north Queensland 2007–2010: 2011/38.
- Parrot, J.F., and Dugas, F., 1980, The disrupted ophiolitic belt of the Southwest Pacific: evidence of an Eocene subduction zone: *Tectonophysics*, v. 66, no. 4, p. 349-372.
- Richards, J., and Cooper, J., 1966, Potassium-argon measurements of the age of basal schists in the British Solomon Islands: *Nature*, v. 211, p. 1251-1252.
- Ridgway, J., Coulson, F., and Arthurs, J., 1987, The Geology of Choiseul and the Shortland Islands, Solomon Islands, HM Stationery Office.
- Schellart, W.P., Lister, G.S., and Toy, V.G., 2006, A Late Cretaceous and Cenozoic reconstruction of the Southwest Pacific region: Tectonics controlled by subduction and slab rollback processes: *Earth-Science Reviews*, v. 76, no. 3-4, p. 191-233.
- Snelling, N.J., Ingram, I.H., and Chan, K.P., 1970, K-Ar age determinations on samples from the British Solomon Islands Protectorate: 17-14.
- Tejada, M., Mahoney, J., Duncan, R., and Hawkins, M., 1996, Age and geochemistry of basement and alkalic rocks of Malaita and Santa Isabel, Solomon Islands, southern margin of Ontong Java Plateau: *Journal of Petrology*, v. 37, no. 2, p. 361-394.
- Veevers, J., 2000, Change of tectono-stratigraphic regime in the Australian plate during the 99 Ma (mid-Cretaceous) and 43 Ma (mid-Eocene) swerves of the Pacific: *Geology*, v. 28, no. 1, p. 47.
- Weissel, J.K., and Watts, A., 1979, Tectonic evolution of the Coral Sea basin: *J.geophys.Res*, v. 84, p. 4572-4582.

Whattam, S.A., 2009, Arc-continent collisional orogenesis in the SW Pacific and the nature, source and correlation of emplaced ophiolitic nappe components: *Lithos*, v. 113, no. 1-2, p. 88-114.

Whattam, S.A., Malpas, J., Ali, J.R., and Smith, I.E.M., 2008, New SW Pacific tectonic model: Cyclical intraoceanic magmatic arc construction and near-coeval emplacement along the Australia-Pacific margin in the Cenozoic: *Geochem.Geophys.Geosyst*, v. 9, no. 3, p. Q03021.

Whittaker, J.M., Mueller, R.D., Leitchenkov, G., Stagg, H., Sdrolias, M., Gaina, C., and Goncharov, A., 2007, Major Australian-Antarctic plate reorganization at Hawaiian-Emperor bend time: *Science*, v. 318, no. 5847, p. 83-86.

Withnall, I.W., and Henderson, R.A., 2012, Accretion on the long-lived continental margin of northeastern Australia: *Episodes-Newsmagazine of the InternationalUnion of Geological Sciences*, v. 35, no. 1, p. 166.

Zirakparvar, N., Baldwin, S., and Vervoort, J., 2013, The origin and geochemical evolution of the Woodlark Rift of Papua New Guinea: *Gondwana Research*.

FIGURE DR3

All errors plotted at the 2σ confidence interval and all data taken from Table DR2

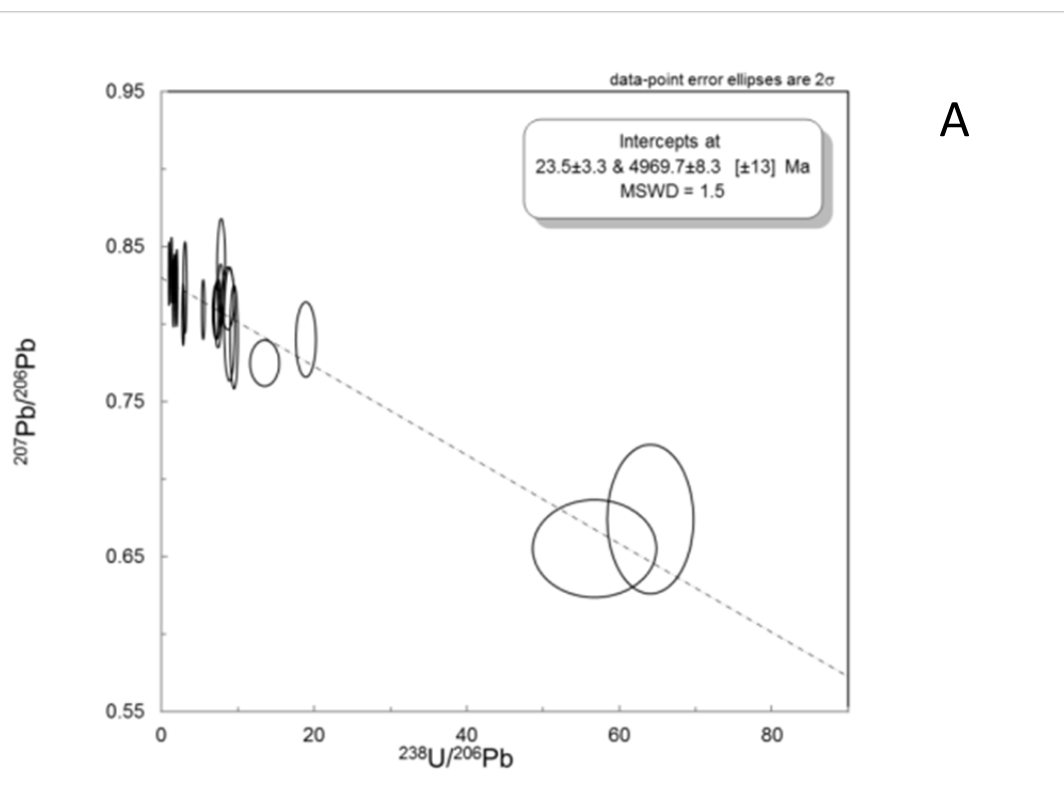
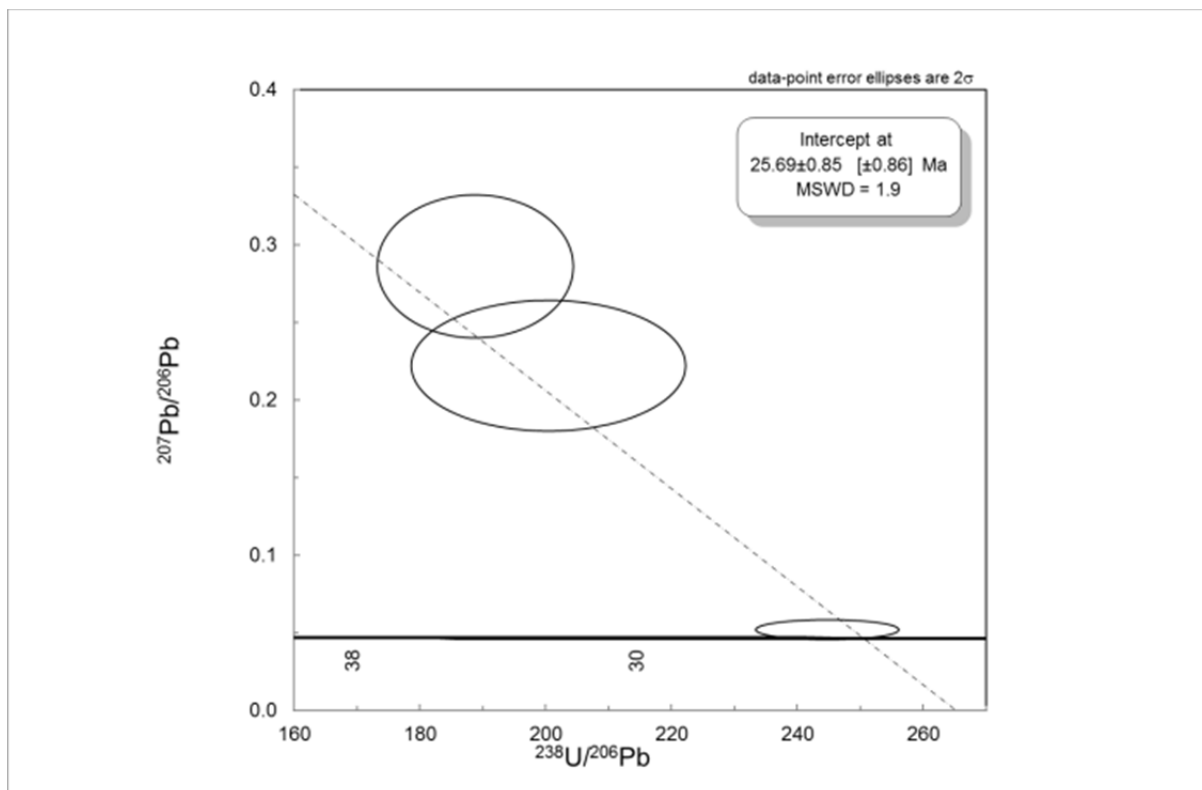
A: Tera-Wasserburg diagram for sample X002 titanite U-Pb data.

B: Tera-Wasserburg diagram for sample UM13B rutile U-Pb data.

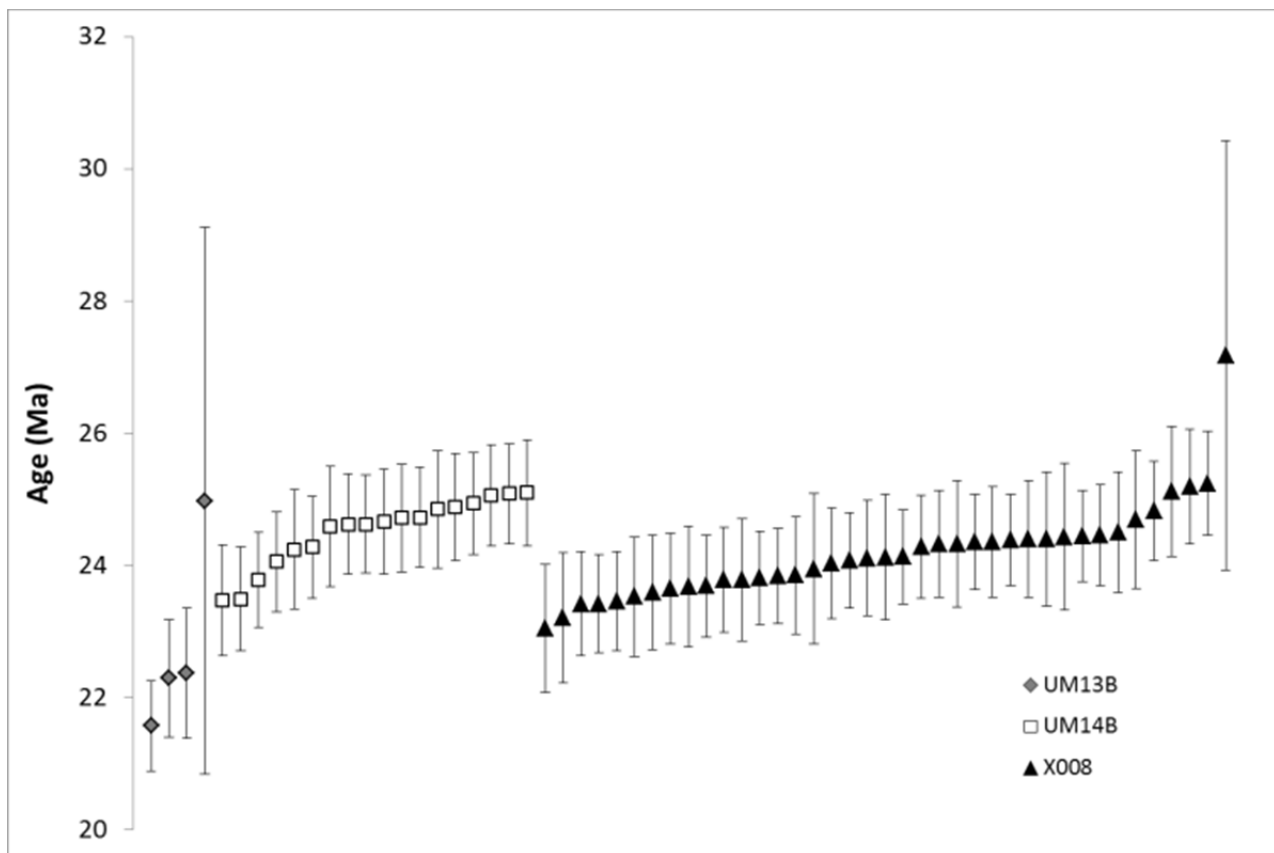
C: U-Pb zircon age distributions for magmatic emplacement populations.

D: U-Pb zircon age distributions for ca 95 Ma populations.

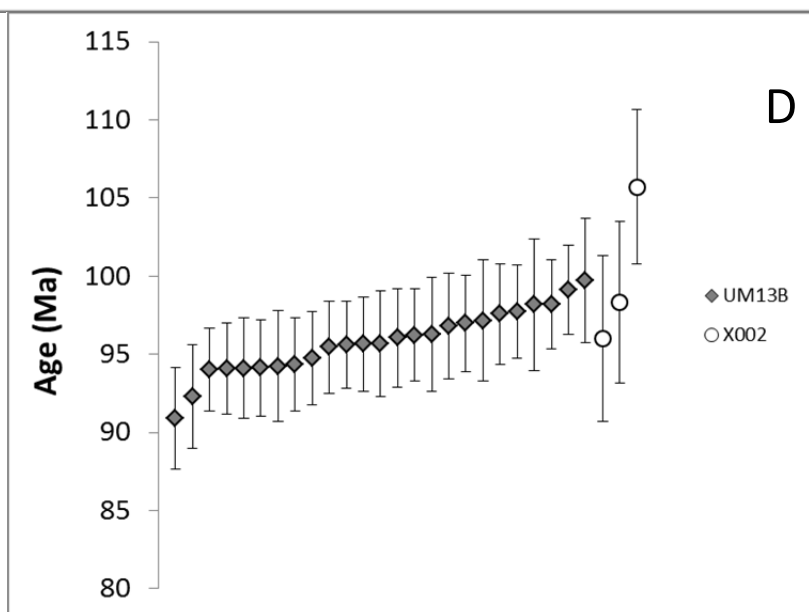
E: Individual sample zircon age frequency histograms



C



D



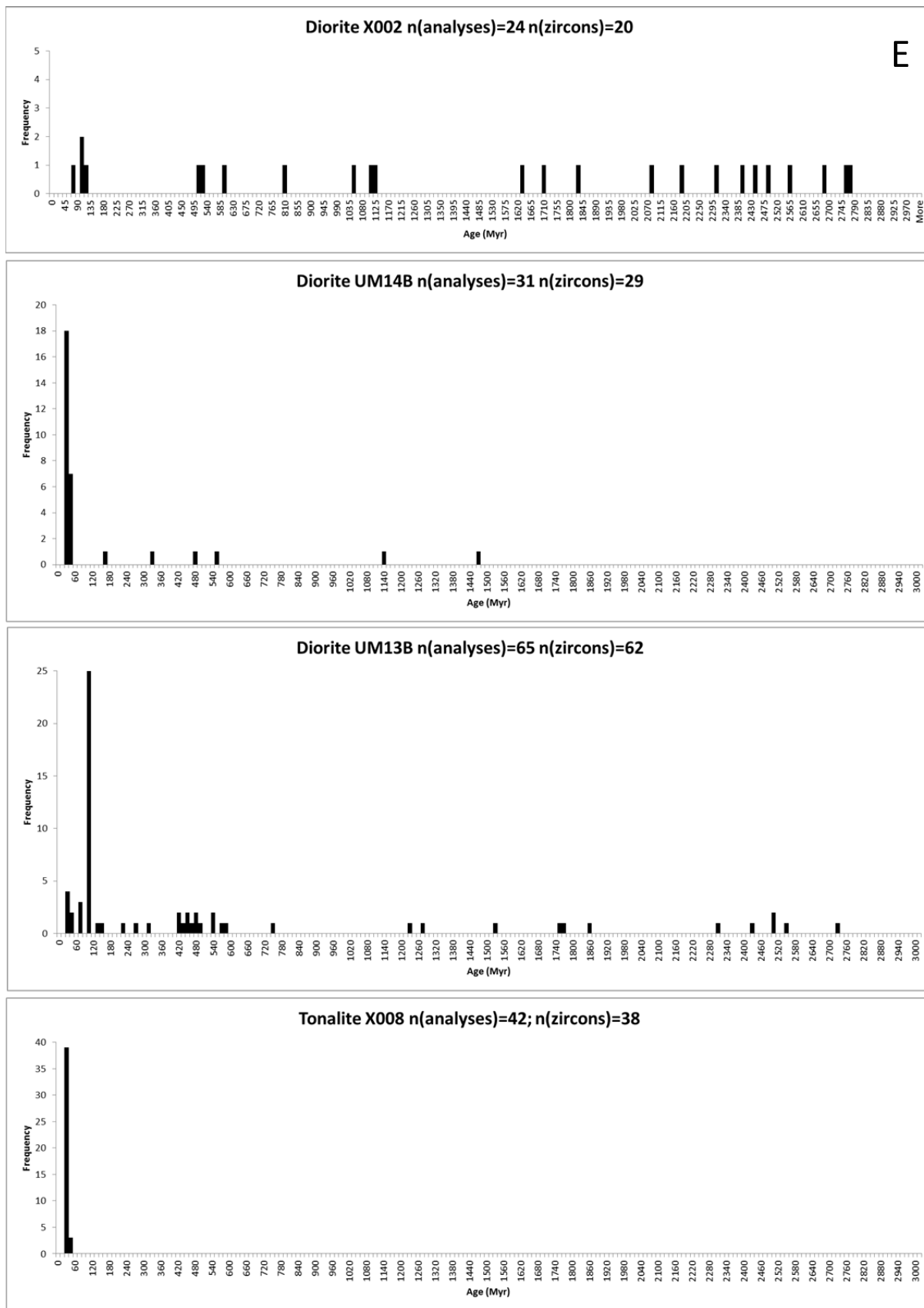


TABLE DR1. Umasani plutonic complex sample details

Sample Name	UTM N	UTM E	Longitude -E (Decimal)	Latitude -S (Decimal)	Rock Type	Alteration	Mineral Phase	Zircons Analysed	Number of Analyses
X002	8961802	584157	159.7664819	-9.39123171	Diorite	Pervasive Chlorite-epidote-albite-pyrite	Zircon + Titane	20	24
UM13B	8961873	581904	159.7459619	-9.390633476	Diorite	Pervasive Chlorite-epidote-albite-pyrite	Zircon + Rutile	62	65
UM14B	8961882	581898	159.7459071	-9.390552195	Diorite	K-felspar halos, Pervasive Chlorite-epidote-albite-pyrite	Zircon	29	31
X008	8962194	583340	159.7590335	-9.387702481	Micro-tonalite	Weak pervasive chlorite	Zircon	38	42

TABLE DR2. Full data table for all U-Th-Pb analyses

Date	Sample	^{204}Pb	f206c	^{206}Pb	^{207}Pb	^{208}Pb	^{232}Th	^{235}U	Th/U	Pb	Th	U	$^{207}\text{Pb}/^{206}\text{Pb}$	1σ	$^{207}\text{Pb}/^{235}\text{U}$	1σ	$^{206}\text{Pb}/^{238}\text{U}$	1σ	Rho	$^{207}\text{Pb}/^{206}\text{Pb}$	2σ	$^{206}\text{Pb}/^{238}\text{U}$	2σ	Disc. %	Disc. %	$^{206}\text{Pb}/^{238}\text{U}$	2σ	Used age	2σ	<10% Disconcordant?		
		cps		cps	cps	cps	cps	cps	ppm	ppm	ppm	%	%	%	%	Ma	Ma	Ma	Ma	Ma	Ma	Ma	Ma	6-38/7-6	6-38/7-35	Cm-Pb corrected	Ma	Ma	Ma			
UM13B -Zircon																																
07/08/2012	UM13B-1-S16	-87	0.00	231821	15288	69966	1234896	16439	0.9	52.6	408	431	0.0655	0.78	1.0892	1.98	0.1206	1.82	0.92	789.9	16.5	734.2	25.2	748.1	20.7	7.1	1.9	733	28.16	748.1	20.7	<10%
07/08/2012	UM13B-1-S17	-20	0.03	229499	18702	34453	379990	29611	0.2	52.1	125	777	0.0817	2.01	0.8611	6.76	0.0765	6.45	0.95	1237.9	39.5	474.9	58.8	630.7	61.6	61.6	24.7	460	61.24	460	61.24	>10%
07/08/2012	UM13B-1-S18	31	0.05	2316	203	602	260303	5495	0.6	0.5	86	144	0.0863	4.53	0.0432	4.95	0.0036	2.01	0.41	1344.9	87.4	23.4	0.9	43.0	4.2	98.3	45.6	22	0.89	22	0.89	>10%
07/08/2012	UM13B-1-S19	37	0.00	95863	5346	26284	880499	11932	0.9	21.7	291	313	0.0560	0.91	0.5239	1.80	0.0678	1.56	0.86	452.7	20.1	423.2	12.8	427.8	12.5	6.5	1.1	423	13.63	423	13.63	<10%
07/08/2012	UM13B-1-S20	-53	0.00	230582	13823	18530	494404	21370	0.3	52.3	163	561	0.0597	0.60	0.7601	1.63	0.0923	1.52	0.93	594.1	12.9	569.0	16.5	574.1	14.2	4.2	0.9	569	18.06	569	18.06	<10%
07/08/2012	UM13B-1-S21	-44	0.01	662845	73958	20750	177414	18537	0.1	150.4	59	486	0.1120	0.64	4.6983	1.64	0.3042	1.51	0.92	1832.5	11.5	1712.0	45.2	1766.9	27.0	6.6	3.1	1697	58.47	1766.9	27.0	<10%
07/08/2012	UM13B-1-S22	55	0.05	12936	1116	3401	970162	20851	0.6	2.9	320	547	0.0844	2.92	0.0618	3.33	0.0053	1.59	0.48	1301.1	56.8	34.1	1.1	60.9	3.9	97.4	43.9	33	1.04	33	1.04	>10%
07/08/2012	UM13B-1-S23	21412	0.63	643842	355410	884963	575168	28374	0.3	146.0	190	744	0.5479	1.90	14.4926	3.41	0.1918	2.84	0.83	4375.6	27.7	1131.3	58.6	2782.5	62.8	74.1	59.3	447	26.92	447	26.92	>10%
07/08/2012	UM13B-1-S24	3038	0.12	430324	66901	142266	901479	41249	0.3	97.6	298	1082	0.1503	2.44	1.8593	2.92	0.0897	1.61	0.55	2348.8	41.7	554.1	17.1	1066.8	37.9	76.4	48.1	491	16.51	491	16.51	>10%
07/08/2012	UM13B-1-S25	-26	0.00	32980	1679	1872	354371	25539	0.2	7.5	117	670	0.0498	1.43	0.0762	2.11	0.0111	1.55	0.74	183.6	33.2	71.2	2.2	74.6	3.0	61.2	4.5	71	2.21	71	2.21	<10%
07/08/2012	UM13B-1-S26	-27	0.02	1664	103	428	240825	3951	0.8	0.4	80	104	0.0643	5.94	0.0314	6.34	0.0035	2.21	0.35	753.0	125.4	22.8	1.0	31.4	3.9	97.0	27.4	22	0.99	22	0.99	>10%
07/08/2012	UM13B-1-S27	-41	0.01	25050	1294	7863	1569130	21096	0.9	5.7	518	554	0.0517	1.60	0.0699	2.23	0.0098	1.55	0.69	271.3	36.8	62.9	1.9	68.6	3.0	76.8	8.3	63	1.95	63	1.95	<10%
07/08/2012	UM13B-1-S28	1379	0.04	708545	60479	73234	640281	87278	0.1	160.7	211	2290	0.0850	2.01	0.8047	2.51	0.0687	1.50	0.60	1315.1	39.1	428.2	12.4	599.5	22.5	67.4	28.6	413	12.76	413	12.76	>10%
07/08/2012	UM13B-1-S29	371	0.11	298189	59458	37756	90247	6849	0.2	67.6	30	180	0.1973	0.76	9.8671	3.08	0.3628	2.99	0.97	2803.7	12.4	1995.3	101.7	2422.4	55.3	28.8	17.6	1808	123.75	2422.4	55.3	>10%
07/08/2012	UM13B-1-S30	117	0.01	50364	3094	8175	240736	5550	0.5	11.4	80	146	0.0620	1.13	0.6486	2.43	0.0758	2.16	0.89	675.3	24.1	471.2	19.6	507.6	19.3	30.2	7.2	468	20.92	468	20.92	>10%
07/08/2012	UM13B-1-S31	-44	0.00	41085	2021	3705	775844	33448	0.3	9.3	256	878	0.0487	1.20	0.0697	2.00	0.0104	1.59	0.80	132.4	28.3	66.6	2.1	68.4	2.6	49.7	2.7	67	2.13	67	2.13	<10%
07/08/2012	UM13B-1-S32	288	0.05	955687	174624	90304	474994	18892	0.3	216.8	157	496	0.1809	0.68	10.6563	1.74	0.4273	1.60	0.92	2660.9	11.3	2293.5	61.6	2493.6	31.8	13.8	8.0	2189	83.89	2493.6	31.8	>10%
07/08/2012	UM13B-1-S33	11960	0.53	423992	200402	468658	204014	25156	0.1	96.2	67	660	0.4690	0.89	9.1634	1.89	0.1417	1.67	0.88	4146.6	13.2	854.3	26.6	2354.5	34.1	79.4	63.7	420	15.29	420	15.29	>10%
07/08/2012	UM13B-1-S35	107	0.08	574347	110391	76190	393968	12079	0.4	130.3	130	317	0.1910	0.73	10.6429	1.74	0.4041	1.57	0.91	2750												

07/08/2012	UM14B-U106	9	0.01	30102	1683	18729	9253961	65489	1.8	6.8	3056	1718	0.0566	1.65	0.0308	2.23	0.0039	1.50	0.67	475.9	36.5	25.4	0.8	30.8	1.4	94.7	17.6	25	0.75	25	0.75	>10%
07/08/2012	UM14B-U107	-24	0.01	20597	1147	8675	4548479	44622	1.3	4.7	1502	1171	0.0554	1.86	0.0296	2.41	0.0039	1.53	0.64	427.0	41.5	24.9	0.8	29.6	1.4	94.2	15.8	25	0.76	25	0.76	>10%
07/08/2012	UM14B-U108	0	0.02	14975	897	4975	2555401	32681	1.0	3.4	844	857	0.0590	1.75	0.0319	2.38	0.0039	1.61	0.68	566.3	38.2	25.2	0.8	31.8	1.5	95.6	20.8	25	0.80	25	0.80	>10%
07/08/2012	UM14B-U109-1	256	0.02	14182	838	1252	359608	21114	0.2	3.2	119	554	0.0594	4.45	0.0465	4.94	0.0057	2.15	0.44	580.8	96.7	36.5	1.6	46.1	4.5	93.7	20.9	36	1.55	36	1.55	>10%
07/08/2012	UM14B-U109-2	20	0.16	166565	30749	13500	203443	13957	0.2	3.7	67	366	0.1812	1.35	2.5879	3.59	0.1036	3.33	0.93	2664.1	22.3	635.3	40.1	1297.2	51.3	76.2	51.0	541	37.47	541	37.47	
07/08/2012	UM14B-U112	111	0.01	15937	791	7483	3952856	34528	1.4	3.6	1305	906	0.0507	1.77	0.0273	2.34	0.0039	1.53	0.65	229.3	40.9	25.1	0.8	27.4	1.3	89.0	8.2	25	0.77	25	0.77	<10%
07/08/2012	UM14B-U113	30	0.01	16046	870	8260	4311379	34009	1.6	3.6	1424	892	0.0571	1.94	0.0305	2.52	0.0039	1.61	0.64	496.7	42.7	24.9	0.8	30.5	1.5	95.0	18.3	25	0.79	25	0.79	>10%
07/08/2012	UM14B-U114	-78	0.01	12090	621	3291	1764868	26254	0.8	2.7	583	689	0.0513	2.28	0.0272	2.81	0.0039	1.65	0.59	253.9	52.4	24.8	0.8	27.3	1.5	90.2	9.2	25	0.81	25	0.81	<10%
07/08/2012	UM14B-U115	-6	0.00	19375	1044	3010	122561	3269	0.5	4.4	40	86	0.0546	1.60	0.3820	2.36	0.0507	1.74	0.74	396.0	35.9	319.1	10.8	328.5	13.2	19.4	2.9	318	11.34	318	11.34	<10%
07/08/2012	UM14B-U117-1	-259	0.02	11182	667	1791	538357	16549	0.4	2.5	178	434	0.0617	5.03	0.0483	5.69	0.0057	2.66	0.47	662.2	107.8	36.6	1.9	47.9	5.3	94.5	23.7	36	1.92	36	1.92	>10%
07/08/2012	UM14B-U117-2	109	0.02	26529	1680	1868	298793	10182	0.4	6.0	99	267	0.0626	1.94	0.2125	7.20	0.0246	6.93	0.96	695.7	41.3	156.7	21.4	195.6	25.3	77.5	19.9	154	21.57	154	21.57	>10%
07/08/2012	UM14B-U118	59	0.01	15123	790	5579	2794934	33712	1.0	3.4	923	885	0.0527	2.15	0.0273	2.67	0.0038	1.59	0.59	317.7	48.9	24.2	0.8	27.4	1.4	92.4	11.7	24	0.76	24	0.76	>10%
07/08/2012	UM14B-U120	49	0.03	49461	3222	21689	11061850	104733	1.3	11.2	3653	2748	0.0665	2.20	0.0363	2.68	0.0040	1.54	0.57	821.4	45.9	25.5	0.8	36.2	1.9	96.9	29.6	25	0.77	25	0.77	>10%
07/08/2012	UM14B-U121	-97	0.01	5039	274	3133	1635310	11279	1.8	1.1	540	296	0.0515	3.06	0.0272	3.57	0.0038	1.85	0.52	262.8	70.2	24.7	0.9	27.3	1.9	90.6	9.5	25	0.91	25	0.91	<10%
07/08/2012	UM14B-U123	47	0.01	8474	474	5219	2541653	18880	1.7	1.9	839	495	0.0574	3.00	0.0301	3.53	0.0038	1.87	0.53	505.0	66.0	24.5	0.9	30.2	2.1	95.1	18.7	24	0.91	24	0.91	>10%
07/08/2012	UM14B-U124	52	0.01	16790	893	8880	3939294	36525	1.4	3.8	1301	958	0.0533	1.89	0.0283	2.41	0.0039	1.51	0.62	340.0	42.7	24.8	0.7	28.3	1.3	92.7	12.5	25	0.74	25	0.74	>10%
07/08/2012	UM14B-U125	-69	0.01	16927	844	6537	3236634	36555	1.1	3.8	1069	959	0.0509	1.91	0.0274	2.50	0.0039	1.60	0.64	235.9	44.2	25.2	0.8	27.5	1.4	89.3	8.5	25	0.80	25	0.80	<10%
07/08/2012	UM14B-U127	115	0.02	14097	854	6267	3039073	31470	1.2	3.2	1004	826	0.0589	2.08	0.0311	2.61	0.0038	1.58	0.61	565.2	45.2	24.6	0.8	31.1	1.6	95.6	20.8	24	0.77	24	0.77	>10%
07/08/2012	UM14B-U130	-46	0.01	11654	589	2834	961025	16860	0.7	2.6	317	442	0.0508	2.04	0.0406	2.62	0.0058	1.65	0.63	229.6	47.2	37.3	1.2	40.4	2.1	83.8	7.7	37	1.23	37	1.23	<10%
07/08/2012	UM14B-U131	22	0.02	17684	1175	6443	2939998	40213	0.9	4.0	971	1055	0.0654	2.32	0.0336	2.85	0.0037	1.66	0.58	786.8	48.7	24.0	0.8	33.6	1.9	97.0	28.5	23	0.78	23	0.78	>10%
07/08/2012	UM14B-U133	-13	0.01	35250	1994	23569	12316230	76919	2.0	8.0	4068	2018	0.0559	1.69	0.0298	2.28	0.0039	1.53	0.67	450.1	37.6	24.9	0.8	29.8	1.3	94.5	16.6	25	0.76	25	0.76	>10%
07/08/2012	UM14B-U134	16	0.00	149830	8311	16503	474982	17104	0.3	34.0	157	449	0.0547	0.79	0.5684	1.73	0.0754	1.54	0.89	400.4	17.6	468.3	13.9	457.0	12.7	-16.9	-2.5	469	15.01	469	15.01	<10%
07/08/2012	UM14B-U135	-94	0.00	211003	16757	50106	532785	9544	0.7	47.9	176	250	0.0792	2.0332	1.82	0.1862	1.61	0.89	1176.6	16.6	1101.0	32.6	1126.7	24.4	1097	38.51	1126.7	24.4	<10%			
07/08/2012	UM14B-U139	133	0.0																													

06/08/2012	X008-2-U18	16	0.03	11497	825	4350	2256810	26007	1.1	2.3	668	602	0.0698	4.63	0.0365	4.92	0.0038	1.67	0.34	922.2	95.1	24.4	0.8	36.4	3.5	97.4	33.0	24	0.79	24	0.79	>10%
06/08/2012	X008-2-U19	75	0.06	6634	611	4968	2345350	14582	2.1	1.4	694	337	0.0908	4.72	0.0504	5.07	0.0040	1.85	0.37	1442.5	90.0	25.9	1.0	50.0	4.9	98.2	48.1	25	0.91	25	0.91	>10%
06/08/2012	X008-2-U20	46	0.02	1773	110	356	207912	4152	0.6	0.4	62	96	0.0641	5.99	0.0323	6.35	0.0036	2.11	0.33	746.2	126.7	23.5	1.0	32.3	4.0	96.9	27.2	23	0.97	23	0.97	>10%
06/08/2012	X008-2-U21	83	0.01	7817	396	2835	1694019	17755	1.2	1.6	502	411	0.0509	2.53	0.0266	3.03	0.0038	1.66	0.55	238.3	58.4	24.4	0.8	26.7	1.6	89.8	8.6	24	0.81	24	0.81	<10%
06/08/2012	X008-2-U22	47	0.02	20928	1234	10961	5484136	46187	1.5	4.3	1624	1069	0.0601	2.63	0.0324	3.03	0.0039	1.51	0.50	606.9	56.8	25.2	0.8	32.4	1.9	95.8	22.3	25	0.75	25	0.75	>10%
06/08/2012	X008-2-U23-1	99	0.00	4160	213	973	549350	9858	0.7	0.8	163	228	0.0487	3.90	0.0245	4.35	0.0037	1.92	0.44	133.1	91.7	23.5	0.9	24.6	2.1	82.3	4.5	24	0.90	24	0.90	<10%
06/08/2012	X008-2-U23-2	-62	0.05	3941	316	1243	552339	8492	0.8	0.8	164	196	0.0857	5.56	0.0470	5.94	0.0040	2.07	0.35	1331.5	107.7	25.6	1.1	46.6	5.4	98.1	45.1	24	1.01	24	1.01	>10%
06/08/2012	X008-2-U25	-78	0.03	11393	813	5734	2401741	24655	1.2	2.3	711	570	0.0714	3.62	0.0397	4.01	0.0040	1.73	0.43	969.3	73.8	25.9	0.9	39.5	3.1	97.3	34.4	25	0.87	25	0.87	>10%
06/08/2012	X008-2-U26	93	0.00	41950	2099	20720	11806970	98458	1.5	8.5	3496	2278	0.0485	1.16	0.0251	1.89	0.0038	1.49	0.79	125.5	27.4	24.1	0.7	25.2	0.9	80.8	4.1	24	0.72	24	0.72	<10%
06/08/2012	X008-2-U28	43	0.00	8640	432	2715	1502843	19867	1.0	1.8	445	460	0.0502	2.44	0.0264	2.89	0.0038	1.56	0.54	205.5	56.5	24.5	0.8	26.4	1.5	88.1	7.3	24	0.76	24	0.76	<10%
06/08/2012	X008-2-U29-1	82	0.01	19368	1109	4554	1450883	29200	0.6	3.9	430	676	0.0575	2.17	0.0456	2.69	0.0058	1.60	0.59	511.7	47.6	37.0	1.2	45.3	2.4	92.8	18.4	37	1.17	37	1.17	>10%
07/08/2012	X008-2-U29-2	257	0.05	30664	2791	11669	3396399	44357	1.0	6.7	1061	1089	0.0857	7.11	0.0705	7.35	0.0060	1.89	0.26	1332.3	137.5	38.3	1.4	69.2	9.8	97.1	44.6	37	1.38	37	1.38	>10%
07/08/2012	X008-2-U29-3	164	0.07	26602	2678	11324	3090141	37357	1.1	5.8	966	917	0.1015	2.24	0.0867	2.72	0.0062	1.54	0.57	1652.1	41.5	39.8	1.2	84.5	4.4	97.6	52.9	37	1.15	37	1.15	>10%
06/08/2012	X008-2-U30	78	0.04	6248	486	3027	1247850	14432	1.1	1.3	369	334	0.0774	3.32	0.0406	3.80	0.0038	1.84	0.48	1132.0	66.2	24.5	0.9	40.4	3.0	97.8	39.4	24	0.87	24	0.87	>10%
07/08/2012	X008-2-U37-1	52	0.02	13983	794	4804	2475969	32113	1.0	3.0	774	789	0.0615	3.60	0.0318	4.09	0.0038	1.94	0.48	656.8	77.2	24.2	0.9	31.8	2.6	96.3	24.1	24	0.92	24	0.92	>10%
07/08/2012	X008-2-U37-2	-19	0.00	9557	459	2823	1604106	22023	0.9	2.1	501	541	0.0474	2.05	0.0246	2.61	0.0038	1.61	0.62	70.5	48.8	24.2	0.8	24.7	1.3	65.7	1.9	24	0.78	24	0.78	<10%
06/08/2012	X008-2-U47	14	0.03	4537	310	1323	693980	10244	0.9	0.9	205	237	0.0677	2.86	0.0355	3.41	0.0038	1.87	0.55	860.6	59.3	24.4	0.9	35.4	2.4	97.2	31.0	24	0.89	24	0.89	>10%
06/08/2012	X008-2-U48	22	0.01	2700	139	541	273369	6123	0.6	0.5	81	142	0.0527	4.55	0.0280	5.02	0.0039	2.11	0.42	314.5	103.6	24.8	1.0	28.0	2.8	92.1	11.5	25	1.04	25	1.04	>10%
06/08/2012	X008-2-U50	-37	0.00	2684	131	965	563682	6271	1.2	0.5	167	145	0.0502	5.30	0.0263	5.77	0.0038	2.28	0.40	203.4	123.1	24.5	1.1	26.4	3.0	88.0	7.2	24	1.11	24	1.11	<10%
	UM13B Rutile																															
08/08/2012	UM13B1-rutile1	-21		2414	1692	3951	1404	1128	0.0	0.3	0	13	0.6742	2.91	1.4509	4.63	0.0156	3.60	0.778	4676.6	42.0	99.8	7.1	910.3	54.2	2.1	89.0	n/a	n/a	n/a		
08/08/2012	UM13B1-rutile2	13032		244362	206868	508279	1372922	2711	6.5	25.3	206	32	0.8198	1.09	72.4307	2.99	0.6408	2.79	0.931	4956.6	15.5	3192.0	138.9	4362.4	58.3	64.4	26.8	n/a	n/a	n/a		
08/08/2012	UM13B1-rutile3	7465		139973	117988	285381	484886	2846	2.2	14.5	73	33	0.8061	1.01	39.3174	2.25	0.3538	2.01	0.894	4932.5	14.4	1952.5	67.4	3753.7	43.6	39.6	48.0	n/a	n/a	n/a		
08/08/2012	UM13B1-rutile4	4452		84166	71408	175667	256358	4779	0.7	8.7	38	56	0.8370	1.51	14.7758	3.14	0.1280	2.75	0.877	4986.1	21.4	776.6	40.1	2800.9	58.0	15.6	72.3	n/a	n/a	n/a		
08/0																																